


Article

Deformation of the Cambro-Ordovician Amdeh Formation (Members 1 and 2): Characteristics, Origins, and Stratigraphic Significance (Wadi Amdeh, Saih Hatat Dome, Oman Mountains)

Frank Mattern ^{1,*}, Andreas Scharf ¹, Pu-Jun Wang ², Ivan Callegari ³, Iftikhar Abbasi ¹, Saja Al-Wahaibi ¹ , Bernhard Pracejus ¹ and Katharina Scharf ³

¹ Department of Earth Sciences, Sultan Qaboos University, Muscat 123, Oman; scharfa@squ.edu.om (A.S.); Iftikhar@squ.edu.om (I.A.); sajasalim995@gmail.com (S.A.-W.); pracejus@squ.edu.om (B.P.)

² College of Earth Sciences and Key-Lab for Evolution of Past Life & Environment in NE Asia (Ministry of Education of China), Jilin University, Changchun 130061, China; wangpj@jlu.edu.cn

³ Department of Applied Geosciences, German University of Technology in Oman, Halban PO Box 1816, Oman; ivan.callegari@gutech.edu.om (I.C.); katharina.scharf@gutech.edu.om (K.S.)

* Correspondence: frank@squ.edu.om

Received: 27 December 2019; Accepted: 16 January 2020; Published: 27 January 2020



Abstract: The Angudan Orogeny affected Cryogenian to earliest Cambrian sedimentary rock formations of the Jabal Akhdar Dome of the Oman Mountains. These rocks were folded and cleaved at 525 ± 5 Ma. We studied the Cambro-Ordovician (Terreneuvian to Darriwillian) Amdeh Formation of the neighboring Saih Hatat Dome to see whether this formation was also affected by the Angudan Orogeny. The Angudan deformation within the Jabal Akhdar Dome is known for its folds and cleavage. Due to age considerations (see above), we studied the folds and cleavages within the two oldest members of the Amdeh Formation (Am 1 and Am 2) in order to compare them with the ones that are known from the Jabal Akhdar Dome to possibly detect Angudan-related deformation in Am 1 and Am 2. Angudan folds of the Jabal Akhdar Dome display fold axes that are oriented NE/SW, but the two lowest members of the Amdeh Formation reveal one set of folds with subhorizontal fold axes that trend NW-NNW/SE-SSE. The lack of Angudan-related folds suggests that the lowest Amdeh Member (Am 1) postdates the Angudan Orogeny. The age of Am 1 is uncertain. Based on our structural results, we consider an upper Terreneuvian age (late stage 2) for Am 1. The folds in Am 1 and 2 are related to the Late Cretaceous–Cenozoic Semail Orogeny (term introduced here). The observed fold vergences (mainly to the W and SW) were caused by shear deformation during descent into the subduction zone by simple shear. The contact between the stratigraphically underlying Hiyam Formation and the Amdeh Formation is generally considered to be an unconformity. We observed a distinct NW/SE-striking deformation zone along the contact of both formations which is located in proximity to the largest observed fold. Tectonically, this contact is defined by the sinistral Wadi Amdeh Fault (name introduced here). The unconformity should be present in the subsurface of the southwestern fault block. Near the contact between the Hiyam and the Amdeh formations, a 20 cm thick unit of reddish cataclasite/tectonic breccia occurs within the basal part of Am 1 which represents a deformed acidic layer or sill. This rock unit could be the first evidence for Cambrian igneous activity.

Keywords: folds; Angudan Unconformity; early Paleozoic volcanism; Ara Rift; Semail Orogeny; Wadi Amdeh Fault

1. Introduction

Recent work in the Jabal Akhdar Dome (Figure 1) has demonstrated two Early Cambrian folding events within Cryogenian to earliest Cambrian rocks [1]. The older deformation episode correlates with the Cadomian Orogeny and the younger episode with the Angudan Orogeny [1]. From Iran (NW) to Afghanistan/NW Pakistan (SE), the Cadomian event is younging from 557 to 516 Ma [1], ([2], their Figure 11a), and the Angudan event dates as 525 ± 5 Ma [3]. The main compression during the Cadomian orogeny was directed NE-SW and NW-SE during the Angudan event [1]. In the course of the Angudan Orogeny, the Cadomian folds were refolded. While the Cadomian folds are associated with shallow, gently dipping slaty cleavage and fold axial planes, the Angudan folds exhibit a steeply dipping system of slaty cleavage and fold axial planes [1].

The Cadomian folds display amplitudes of 5 to 50 m and low-dipping axial planes ($10\text{--}30^\circ$). The Angudan folds are open to close with much larger amplitudes and wavelengths ranging from several hundred meters to 3 and 5 km, respectively. These younger folds exhibit steeply dipping to vertical axial planes striking ENE and fold axes that plunge either $\sim 50^\circ$ to the ENE or $\sim 30^\circ$ to the WSW [1].

We studied the folds of the 3.4 km thick Amdeh Formation of the Saih Hatat Dome (Figure 1) which has been considered to be Ordovician in age [4]. Recently, it was suggested that the five members of the formation (Am 1 to Am 5) can be correlated with subsurface formations to the SSW to the interior of Oman ranging from the Cambrian to the Middle Ordovician (Figure 2) ([5], their Figure 2). However, correlation of the oldest Amdeh Member (Am 1) is less certain than for the other Amdeh members (Figure 2). This member may or may not partly correspond to the Fortunian (Lower Terreneuvian) Karim Formation (Figure 2).

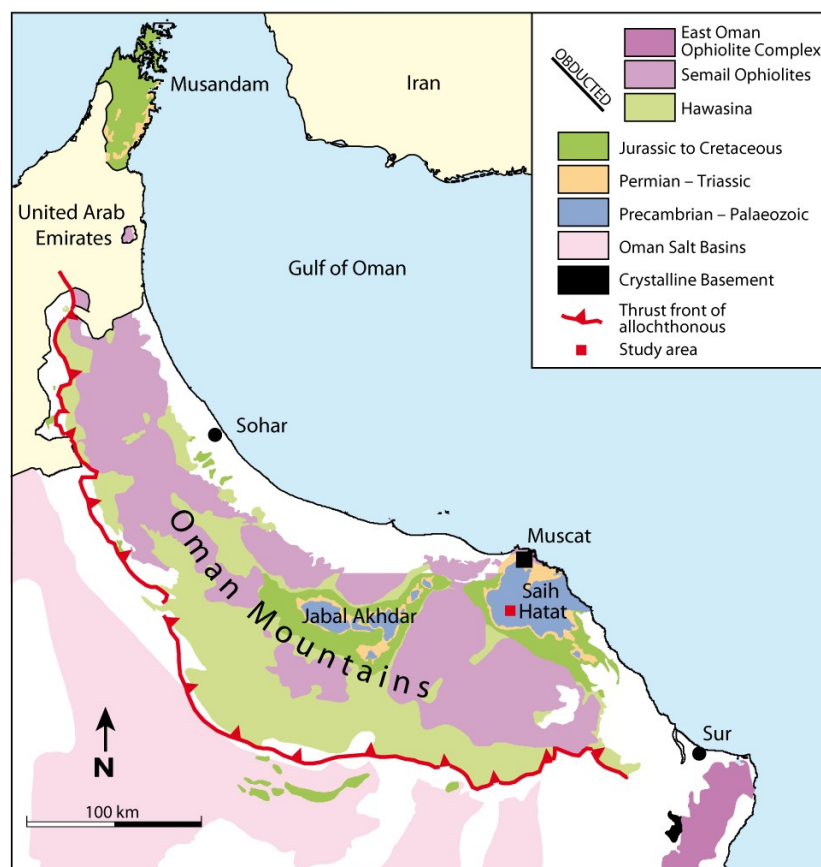


Figure 1. Geological map of the Oman Mountains and position of the study area, drawn after [6]. Note the dome structures of the Jabal Akhdar and Saih Hatat areas.

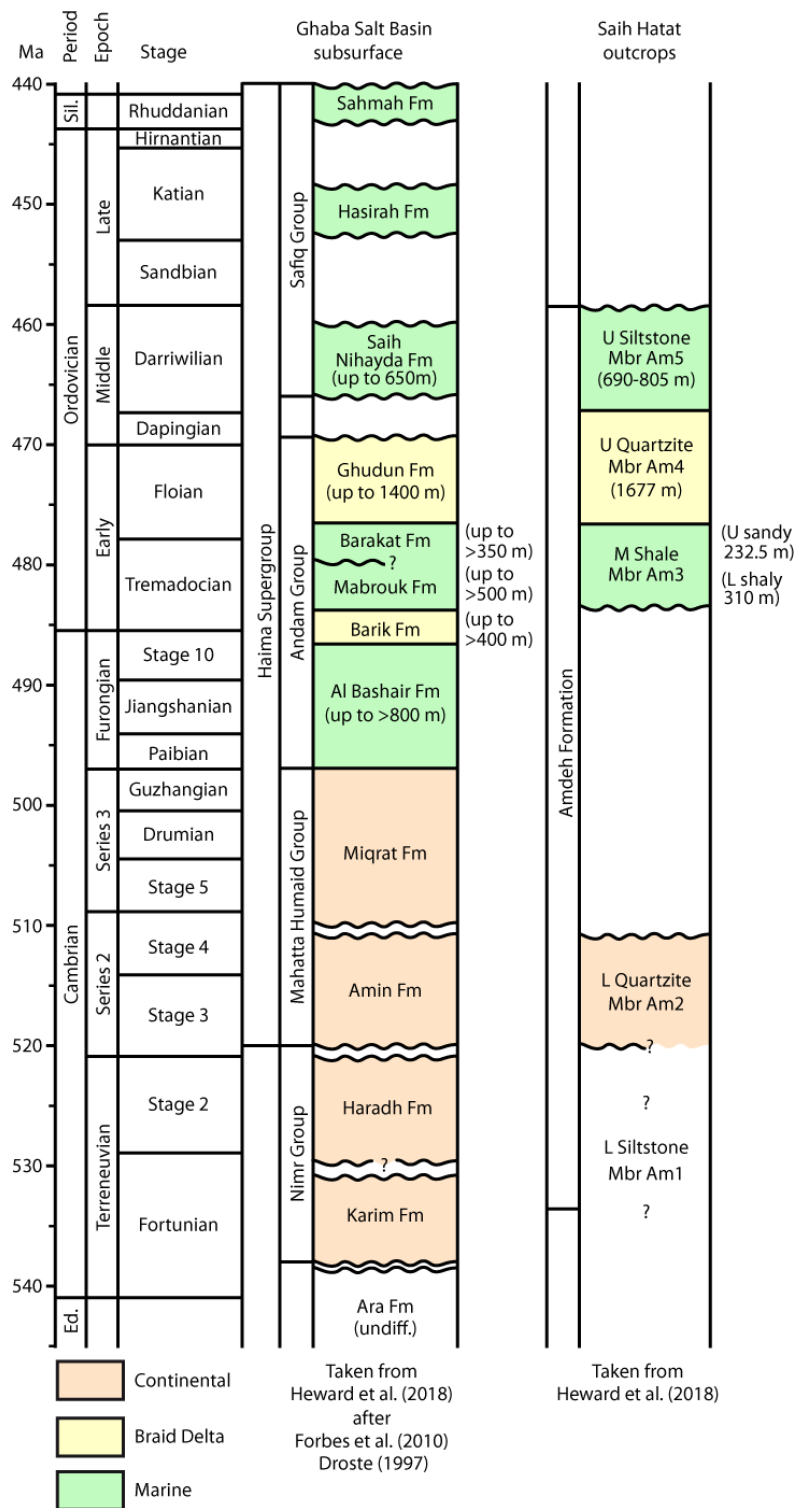


Figure 2. Lateral correlation of the Amdeh Formation (Saih Hatat Dome) with lithologically similar units in the subsurface of Oman (Ghaba Salt Basin), drawn after [5]. Note that the correlation of Am 1 is less certain than that of Am 2–Am 5.

The primary stratigraphic contact between the Amdeh Formation and the underlying Hiyam Formation is an unconformity [4]. This contact displays in most cases deformation to varying degrees [4]. The unconformity of [4] seems to correlate with the Angudan Unconformity which has been introduced and established for central east Oman [7–9].

The overall fold style of the Saih Hatat area is characterized by overturned to recumbent folds [10] or regional isoclinal folds [11], respectively (see also [12]). This deformation is related to Late Cretaceous active margin tectonics which include the obduction of the Semail Ophiolite (e.g., [10,11]). The study area occupies a structural position within the upper limb of a regional recumbent isoclinal fold, distant from the fold closure which is located to the NE ([4], their Figure 2).

Since there is evidence for two Early Cambrian folding events in the Jabal Akhdar area [1] and the possibility of a lower Cambrian age of the Amdeh Formation (Figure 2) [5], we want to determine whether the two oldest Amdeh members show the same fold pattern as the Cryogenian to earliest Cambrian rocks of the Jabal Akhdar Dome. If the lower Amdeh members would have experienced the same tectonic evolution as the Cryogenian to earliest Cambrian rocks of the Jabal Akhdar area, we could demonstrate that the Saih Hatat Dome was also affected by the Cadomian and/or Angudan orogenies, and the age of the Amdeh Formation would include a corresponding early Cambrian age. If none of the Early Cambrian deformation intervals could be detected, the oldest Amdeh members would have to postdate the Angudan Orogeny and deformation would have to be attributed to the Late Cretaceous active margin tectonics. To solve these issues, we studied folds within the lowest two Amdeh members in the western part of the Saih Hatat Dome.

Furthermore, we studied the contact between the Hiyam and Amdeh formations as it is located close to the largest fold element that we encountered (syncline of Figure 3) to clarify the stratigraphic and tectonic nature of the contact. If the Angudan unconformity is present in the study area, Angudan-related folds should not exist in the overlying Amdeh Formation, not to mention the even older Cadomian folds. In the case that the folds of the Amdeh Formation are not related to the Cadomian and Angudan events, we want to understand if and how they are related to the mountain building processes that led to formation of the Oman Mountains since the Late Cretaceous.

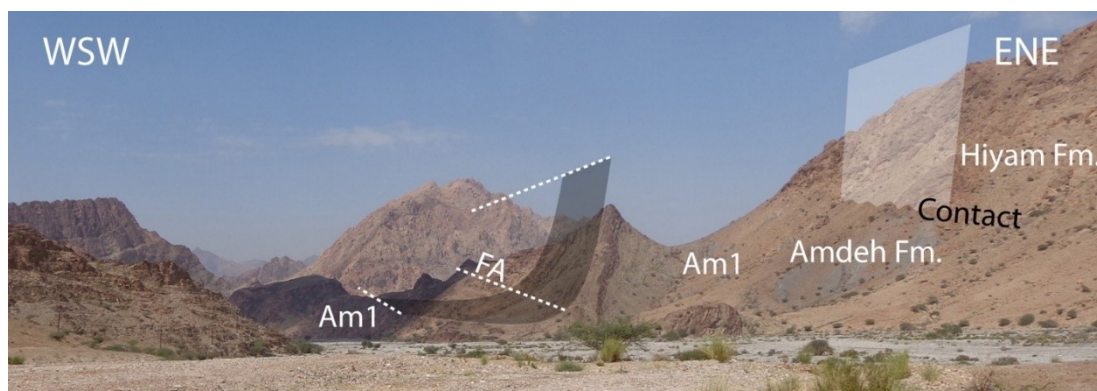


Figure 3. Contact between the Amdeh and Hiyam formations. The contact is marked by the sinistral Wadi Amdeh Fault (dashed white line). Note the slickenlines between the two black dashed lines. The two white arrows point to the red cataclasite/tectonic breccia in close proximity to the fault. Note that the red cataclasite/tectonic breccia is obliquely oriented to the fault, being in contact with the fault in the foreground and separated from the fault in the background. Coordinates of the fault: $23^{\circ}19'45.12''\text{N}/58^{\circ}23'43.95''\text{E}$.

We will summarize our field data related to the folds and deformation at the Hiyam and Amdeh contact. Our interpretations will focus on comparing the fold data of the Amdeh Formation with those of the Cadomian and Angudan folds of the Jabal Akhdar Dome and the possible maximum stratigraphic age of the Amdeh Formation. We will also suggest a deformation path for Am 1 and Am 2 of the study area.

2. Geological Setting

The Oman Mountains contain a diverse association of thick Neoproterozoic to Neogene carbonates and siliciclastics, as well as some volcanic rocks. This succession was affected by various Phanerozoic deformation intervals. Neoproterozoic and Early Paleozoic rocks only crop out in the cores of the large Jabal Akhdar and Saih Hatat domes (Figure 1), and it has to be noted that the stratigraphy of these formations differs between the two domes (e.g., [13–19]) as summarized in Figure 4. All pre-Permian formations shown in Figure 4 (in light gray) for the Jabal Akhdar Dome were subjected to Cadomian folding and Angudan refolding [1].

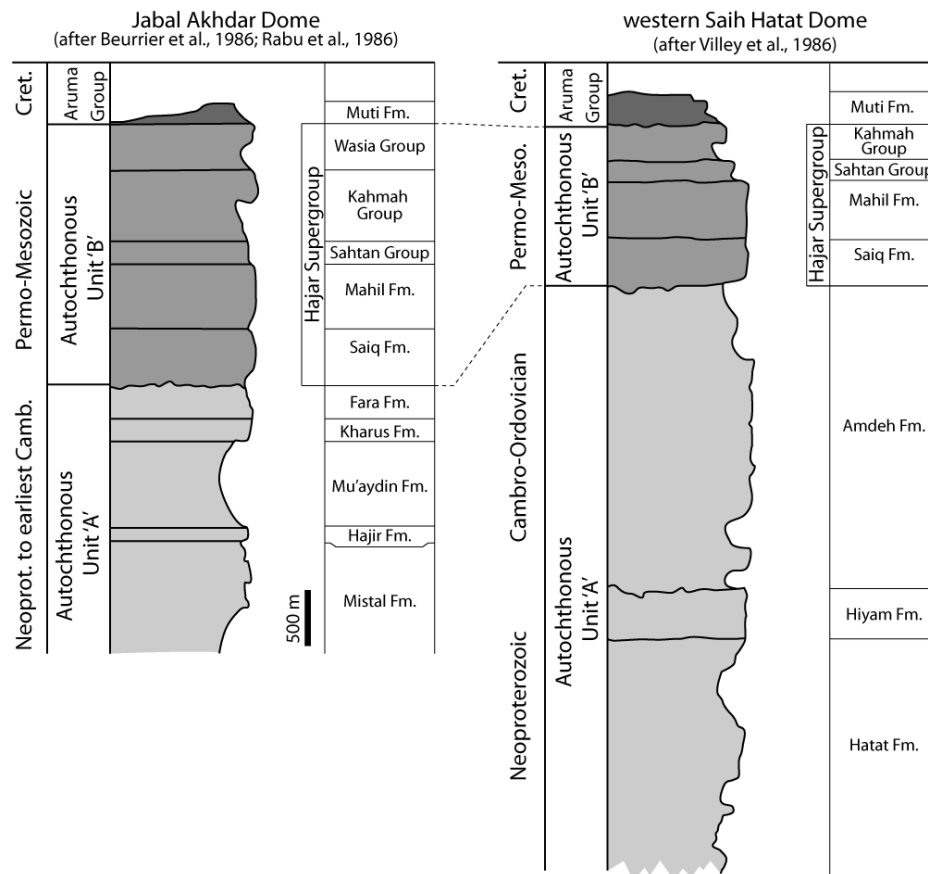


Figure 4. Different stratigraphies of the Jabal Akhdar and Saih Hatat domes, drawn after [13–15]. Note the pronounced differences among the Early Paleozoic formations. The lowermost five formations of the Jabal Akhdar Dome (in light gray) were affected by the Cadomian and Angudan orogenies. The scale applies to both logs.

The earliest Phanerozoic deformation of the area of the Oman Mountains is the Early Cambrian Cadomian Orogeny [1]. The age of the Cadomian Orogeny postdates the Fara Formation (Figure 4). Considering U-Pb ages of zircons from volcanic layers of the Fara Formation by [20,21], the top of the Fara Formation dates as 542 Ma.

The Cadomian Orogeny was followed by the slightly younger but still Early Cambrian Angudan Orogeny [9] which is related to the collision of East and West Gondwana (~540–520 Ma; [3,6,7] ([9], his figure 6a) [22–24]. According to the compilation of [3], the Angudan event occurred 525 ± 5 Ma ago. Two K/Ar crystallization ages of chlorite of 329 ± 11 and 321 ± 10 Ma from the Neoproterozoic Mu'aydin Formation of the Jabal Akhdar Dome [13] coincide with the Late Paleozoic Hercynian Orogeny centered in Europe, (e.g., [25,26]). However, the idea of the Hercynian Orogeny being present in the Oman Mountains appears to be obsolete (see review in [1]). At that time, the study area and the Arabian Plate were only affected by arch formation as depicted by [27] and [28] and block faulting [13,14]. Instead of

the Hercynian Orogeny the breakoff of the Cimmeria Superterrane from Gondwana took place [29], regionally represented by the Lut and Afghan terranes [30], and one can consider a major regional thermal event [31].

During the Late Paleozoic, northern Oman was affected by the Permian Pangea Rifting e.g., [32–34]. Together with the breakoff of Cimmeria, rifting of Pangea caused a major unconformity, above which the ~2 km thick Permo-Mesozoic Hajar Supergroup accumulated. These sediments are mostly of shallow marine facies, dominated by carbonates, representing the Arabian shelf.

Rifting led to drifting and creation of the Tethys Ocean also referred to as the “Neo-Tethys Ocean”. For early drift stage paleogeographic maps, see [35] as well as [36]. From this ocean, the famous Semail Ophiolite originates which is widely and well-exposed in the Oman Mountains. The Semail Ophiolite consists mainly of igneous rocks, representing oceanic mantle and crust which formed in the Semail Basin which opened at a new spreading center ([36] and sources therein) at the southern margin of the Tethys Ocean around 96 Ma [37]. The ophiolite was obducted onto the continental Arabian Plate from the northeast due to Late Cretaceous ocean closure and caused folding. Fold axes of the two domes generally trend parallel to the orientation of the Oman Mountains which is NNW/SSE or NW/SE, respectively (Figure 1 for overview). Deep marine Tethys sediments of Permo-Mesozoic age were also obducted (Hawasina Allochthon) along with the Semail Ophiolite. The Hawasina sediments occupy a structural position below the ophiolite. The obducted rock masses overthrust the Arabian shelf deposits of the Hajar Supergroup, and their combined load formed the Aruma Foreland Basin. The Late Cretaceous sediments of this foredeep (Aruma Group) were also overthrust by the obducted rock units [38–44].

During Late Cretaceous obduction of the Tethyan rocks, parts of the northeastern margin of the Arabian Plate, including the Saih Hatat area, were subducted and metamorphosed under HP/LT conditions, reaching the glaucophane-eclogite facies conditions (e.g., [12,36,45]). The autochthonous Amdeh Formation of the western Saih Hatat Dome was exposed to this metamorphism at conditions of the deep anchizone to pumpellyite/lawsonite zone [12,36,46]. This metamorphism is of Cenomanian age, and there is evidence for exhumation and retrograde metamorphism (review in [36]. By comparison, only the NE corner of the Jabal Akhdar Dome was affected by pumpellyite/lawsonite facies conditions. Towards the SW, the deep and the upper anchizones follow, indicating an overall lower metamorphic grade as in the Saih Hatat Dome [36]. Evidently, the rocks of the Saih Hatat area were subducted to greater depths than those of the Jabal Akhdar region (e.g., [36,47,48]).

Following obduction, the flanks of the two domes (i.e., the obducted rocks) were covered by fluvio-deltaic clastic rocks of the Late Cretaceous Al-Khod Formation and Cenozoic shallow marine carbonates, [16,49]. Obduction was followed by unsteady exhumation of the Saih Hatat and Jabal Akhdar domes during the Late Cretaceous and Cenozoic [47,48,50,51]. Doming was associated with extension related to gravitational collapse [47,48,52–55]. Extension led to the formation of large-scale listric normal faults bounding the flanks of the domes [54]. A paleostress analysis was carried out by [53] for the Late Cretaceous to the Pliocene for areas to the north, and west of the Saih Hatah Dome, not including the study area (Figure 5). In reference to the important Semail Ophiolite, we introduce the term “Semail Orogeny” to summarize all mountain building processes that produced the modern Oman Mountains (or “Hajar Mountains”) since the Late Cretaceous.

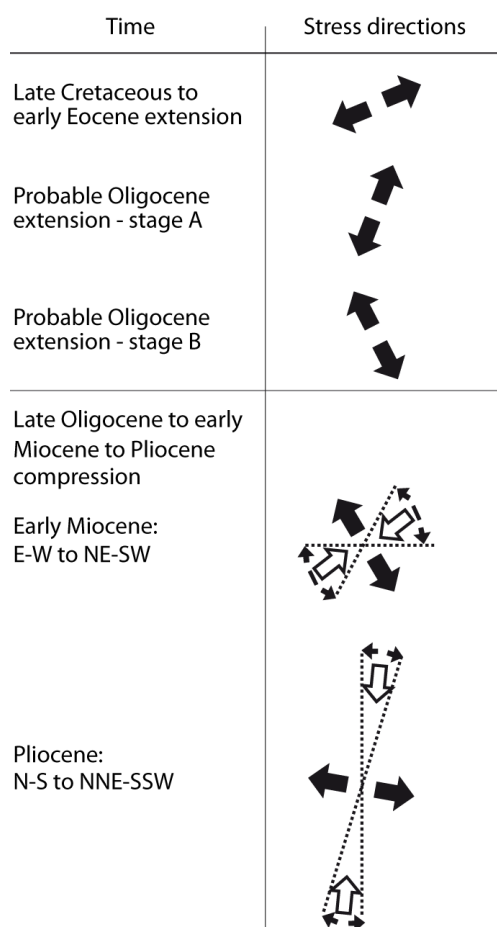


Figure 5. Overview of the changing Late Cretaceous to Pliocene paleostress directions of the eastern Oman Mountains, drawn after [53].

3. Methods

We studied the folds of Am 1 and Am 2 and determined the orientation of the fold axes, either by measuring them directly or by reconstructing the intersection linears of the fold limbs. For optimum accuracy, we used a fabric compass after [56] for the structural measurements. Accordingly, our fabric measurements indicate (dip direction/dip angle) or (plunge direction/plunge angle). We measured folds of different sizes, recorded the fold style (interlimb angle), and inspected the studied outcrops for possible refolded folds. We plotted the fold axes as poles in a Schmidt net and decided by the tightness of the obtained point distribution that 30–40 fold axes represent a sufficiently meaningful data set. Focal linears of fold axes clusters were determined with Gefuege 3 by [57]. Our investigation of the contact between the Hiyam and Amdeh formations required the analysis of five thin sections, three XRD samples, and one XRF sample. From the XRF sample, we produced six measurements.

4. Outcrops and Lithologies of Am 1 and Am 2

We studied natural outcrops of the lower Amdeh Formations (Am 1 and Am 2) in the type area around Wadi Amdeh within the western part of the Saih Hatat Dome (Figure 1). These outcrops mainly occur in Wadi Amdeh and its southern tributary, Wadi Qahza. Some outcrops are also located in a small western tributary of Wadi Qahza.

The lower part of Am 1 consists of metasiltstone with intercalated fine-grained quartzites and some conglomerates. The crystal size of the metasiltstones exceeds that of phyllites. The metasiltstones are mica-bearing, quartz-rich schists. Towards the top, the grain size increases within Am 1. The upper part of Am 1 is characterized by metaturbidites (some conglomeratic) and conglomeratic metadibrites.

Am 1 lacks metashale partings and is known as the “Lower Siltstone Member” with a thickness of 240 m [4].

The lower part of Am 2 displays monotonous quartzites with rare ripple marks. Towards the top, ripple marks of various kinds become very frequent. The upper part of Am 2 also exhibits frequent cross-bedding and flat-bedded quartzite, as well as occasional sand volcanoes. Am 2 also lacks metashale partings. It is referred to as the “Lower Quartzite Member” and measures 253 m in thickness [4].

The contact between the Hiyam and Amdeh formations was studied on the northeastern valley flank of Wadi Amdeh (Figure 6; coordinates 23°19'45.12" N/58°23'43.95" E, 170 m above valley floor). The upper part of the Hiyam Formation consists of shallow marine limestones which have been widely dolomitized and partly silicified. At the contact, the Amdeh Formation is represented by Am 1 displaying a monotonous quartz-rich siltstone succession with some interbedded sandstone layers and some reworked pebbles and cobbles of the underlying Hiyam Formation.

5. Results

5.1. Folds

We measured 12 folds in Wadi Amdeh, 16 in Wadi Qahza, and eight in the western tributary of Wadi Qahza (Figure 6). The folds are all of meter-scale size except for the much larger syncline depicted in Figure 3. The folds display a harmonious fold style. Most folds exhibit (1) open interlimb angles, (2) axes plunging to the SE-SSE (Figure 7A), (3) steep fold axial planes (Figures 7B and 8A), and (4) the preferred vergence to the W and SW. There are no refolded folds. It is not uncommon for the folds to display thickened hinge areas and thinned limbs (Figure 8A,B).

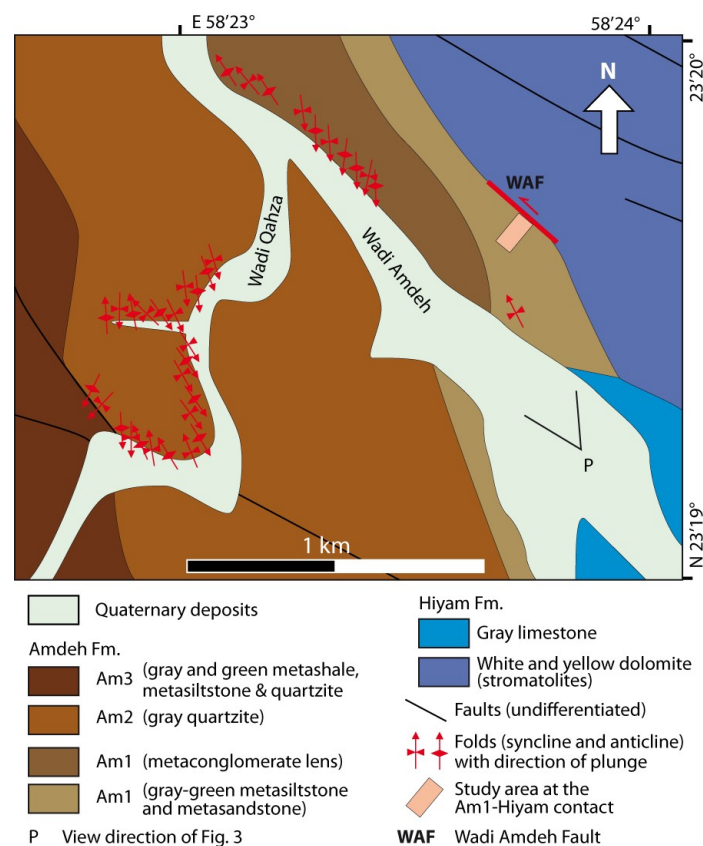


Figure 6. Geological map of the study area with fold locations and location of the contact between the Hiyam and Amdeh formations. Note that the faults in the Hiyam Formation strike similarly to the Amdeh Fault. Partly drawn after [15].

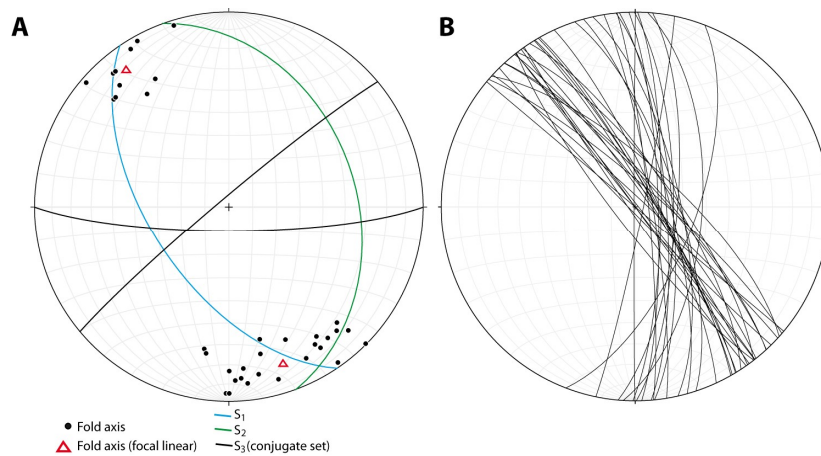


Figure 7. Schmidt nets with equal lower hemisphere projection. (A) Orientation of the 36 fold axes in Am 1 and Am 2, as well as representative S₁ (Am 1 and 2), S₂ and S₃ (Am 1) values. There is a clear geometric relationship between the fold axes on the one hand and S₁, S₂, and S₃ on the other hand. S₁ and S₂ strike approximately parallel to the fold axes while S₃ strikes perpendicularly to the fold axes. (B) Orientation of the fold axial planes of the 36 folds.

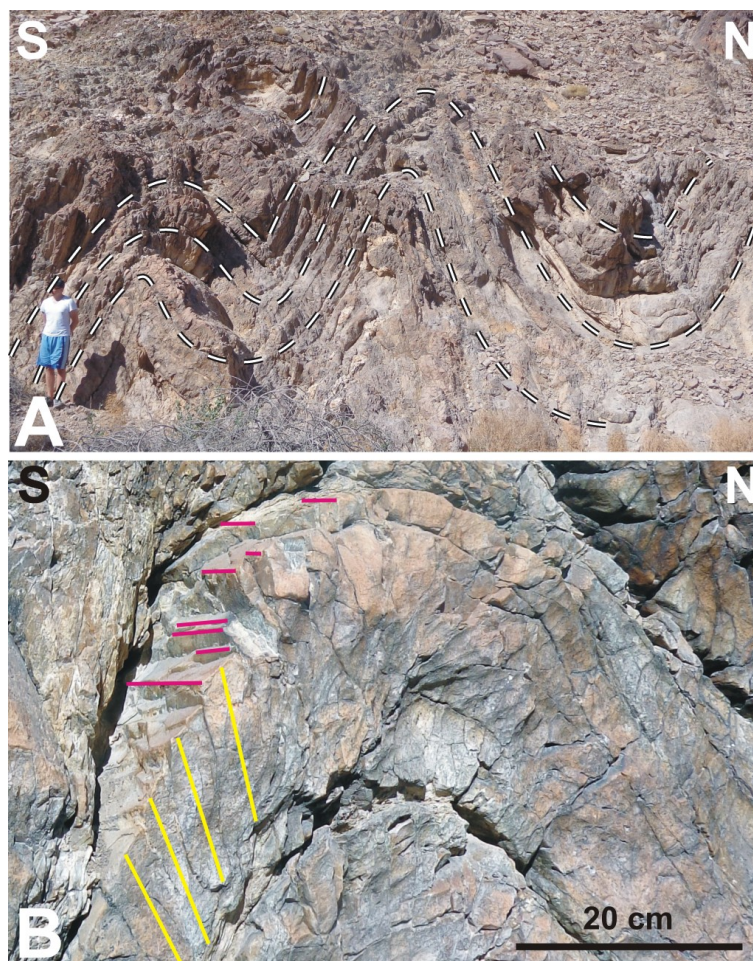


Figure 8. Folds in quartzites of Am 2 with thickened hinge areas and thinned limbs in Wadi Qahza. (A) Typical open folds with vertical or steeply dipping fold axial planes. The folds are clarified by white dashed lines. (B) Anticline with bedding and fold-related cleavage (S₁). The steeply dipping cleavage is marked by yellow lines. The intersection lineations between bedding and cleavage (indicated by red lines) are parallel to the fold axes. Coordinates: 23°19′29.62″ N/58°22′58.52″ E.

In line with the preferred steeply dipping orientation of the fold axial planes (Figure 7B), the cleavage planes also dip steeply (Figure 8B). Some outcrops expose this widely spaced and steeply dipping cleavage and reveal that it is related to folding as their intersections with bedding surfaces produce lineations that are parallelly oriented to the fold axes (Figure 8B).

Generally, the trend of the fold axes parallels the local and regional orientation of the Oman Mountains [58] and the long axis of the Saih Hatat Dome [15,53]. The plot of the determined fold axes (Figure 7A) also reflects that. The folds lack slip features, and most of the fold axial planes are steeply dipping (Figure 7B). The trend of the Amdeh fold axes (Figure 7A) indicates the orientation of the shortening direction which is 240/060°.

5.2. Contact between the Hiyam and Amdeh Formations

The bedding of Am 1 (S_0) is (237/67). Am 1 displays three cleavage systems (Figures 7A and 9). The attitude of S_1 is (236/57) and, thus, similar to that of S_0 . S_1 is a closely spaced (mm scale) slaty to schistose cleavage, displaying little orientational scatter (Figure 9A). S_2 dips more gently with scattered orientations (Figure 9A,B). Their focal orientation is (070/35; Figure 7A). It is a widely spaced (up to several cm) crenulation cleavage. S_3 is a fracture cleavage (spaced cleavage).

This steeply dipping cleavage system (Figures 7A and 9B) is represented by two conjugate sets: (320/86) and (140/80). The intersection of both sets with each other and with the trend of the fold axes creates a highly symmetric system (axial symmetry) of equivalent angles (Figure 7A), typical for a fold-related conjugate cleavage system.

Approaching the contact between the Hiyam and Amdeh formations from the wadi (i.e., from the W; see Figure 3) towards the base of Am 1, bedding becomes slightly steeper from (225/64) to (245/70). Within a 20 m wide zone adjacent to the contact a distinct deformation zone exists displaying an increased intensity of deformation towards the contact as expressed by the occurrence of (1) quartz veins, which parallel S_0 and/or S_1 , (2) boudins, (3) gently dipping quartz-filled veins, (4) widened and steeply dipping calcite-filled faults (260/79) which are paralleled by arrays of widened, right-stepping Riedel shears that are also calcite-filled, (5) sheared and rotated bedding and cleavage fabrics, as well as (6) a cataclasite/tectonic breccia. The contact itself is marked by a large slickenside with horizontal slickenlines. The related fault parallels the trend of Wadi Amdeh in this segment and is referred to here as the “Wadi Amdeh Fault” (name introduced here).

The quartz veins, which parallel S_0 and/or S_1 , have a lateral extent of centimeters to decimeters. Epidote is associated with these veins which are dragged by S_2 .

The boudins in this distinct deformation zone are mainly reworked beige dolostone clasts from the Hiyam Formation. The stretched clasts are embedded in metasilstone to metasandstone matrix and are interpreted to represent clasts within matrix-supported metadibrites. The clasts are roughly parallelly oriented. Stretching is manifested in symmetric and some asymmetric boudins. The latter are associated with Riedel shears (Figure 10). The stretching direction of the clasts is shown in Figure 10, as well as an asymmetric boudin indicating the top-to-the-NE transport. The scatter of the plunge angle values is attributed to different original shapes of the clasts and their original position in the sediment. The stretching directions are perpendicular to the trend of the fold axes and parallel to the transport direction of the folds (vergences) but with the opposite transport polarity.

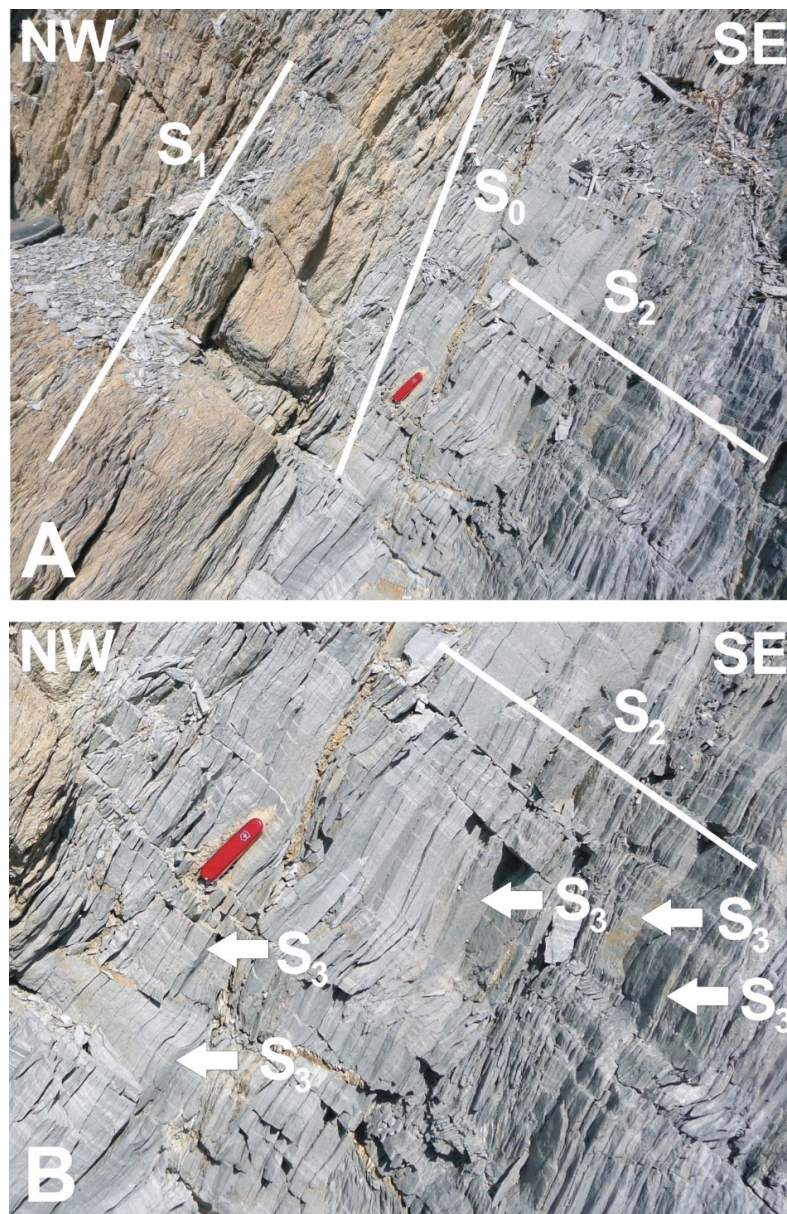


Figure 9. S_0 and cleavage sets in Am 1. The outcrop shows two lithologies. In the upper left area is beige sandstone, and the rest is gray siltstone. Red pocket knife for scale is in the same position in both photographs. (A) Closely spaced S_1 cleavage with little orientational scatter. The orientation of S_1 is subparallel to S_0 (bedding). S_1 is more widely spaced in quartzites (Figure 8B). S_2 is more widely spaced than S_1 with some orientational scatter. (B) Detail of Figure 9A, showing S_2 and S_3 . S_3 is indicated by white arrows whose heads are pointing to individual S_3 surfaces.

The Riedel shears of the calcite-filled fracture system indicate sinistral slip (Figure 11). The attitude of the fault shown in Figure 11 is (263/79). Individual shear veins are oriented (224/67) and intersected/segmented by S_3 . Shearing ensued approximately in N-S direction.

The attitude of the gently dipping quartz-filled veins is shown in Figure 12. Most of these veins follow S_2 or display a similar orientation to S_2 (Figure 12). The thickness of these veins is ≤ 3 cm. The veins are not folded and are not cross-cut by any cleavage. They display some fractures and contain minute calcite shear veins (veins in veins) that are ≤ 1 mm thick with a lateral extent of ≤ 1 cm. These veins are very numerous in the distinct deformation zone close to the contact between the Amdeh and

Hiyam formations. Isolated from these veins we found one thicker quartz vein (10 cm thick) with a corresponding attitude occurring in 350 m distance to the south but still within Am 1.

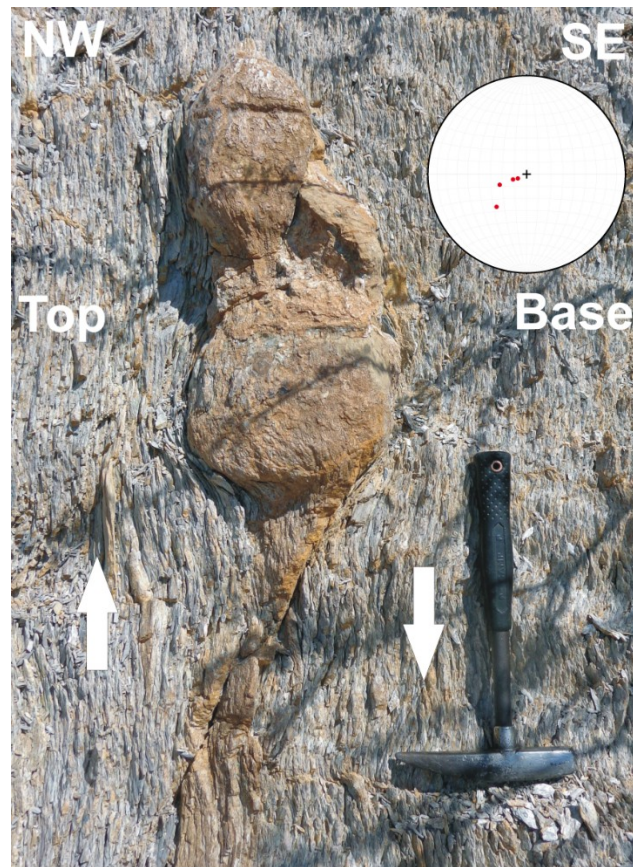


Figure 10. Boudin associated with Riedel shear (left of the hammer). The Riedel shear indicates top-to-the-NE transport. The outcrop is a steeply inclined surface. The Schmidt net shows the stretching direction of four measured boudins.

The sheared and rotated bedding and cleavage fabrics occur within a zone 5–10 m south of the Wadi Amdeh Fault. Even closer to the fault, the cataclasite/tectonic breccia is exposed (Figure 13). It is a 20 cm thick, reddish layer (sill) with a vertical attitude of mainly fine-grained material occurring on the southwestern fault block which features the Amdeh Formation (Figure 13). This unit does not mark the contact between the Hiyam and Amdeh formations as it is obliquely oriented with respect to the Hiyam Formation or the Wadi Amdeh Fault, respectively (Figure 13). Reddish rocks are neither known to occur in Am 1 and Am 2 nor in the upper part of the Hiyam Formation. Thin section evidence shows that it is a cataclasite/tectonic breccia. This rock unit lacks linear structures that could be observed in the field. Under the microscope foliation, flow fabrics, S-C fabric, brittlely sheared mineral grains, as well as porphyroblast-like objects can be identified (Figure 14A–D). These features indicate that deformation conditions may have reached the brittle-ductile transition. The compositional details of this rock unit are summarized below.

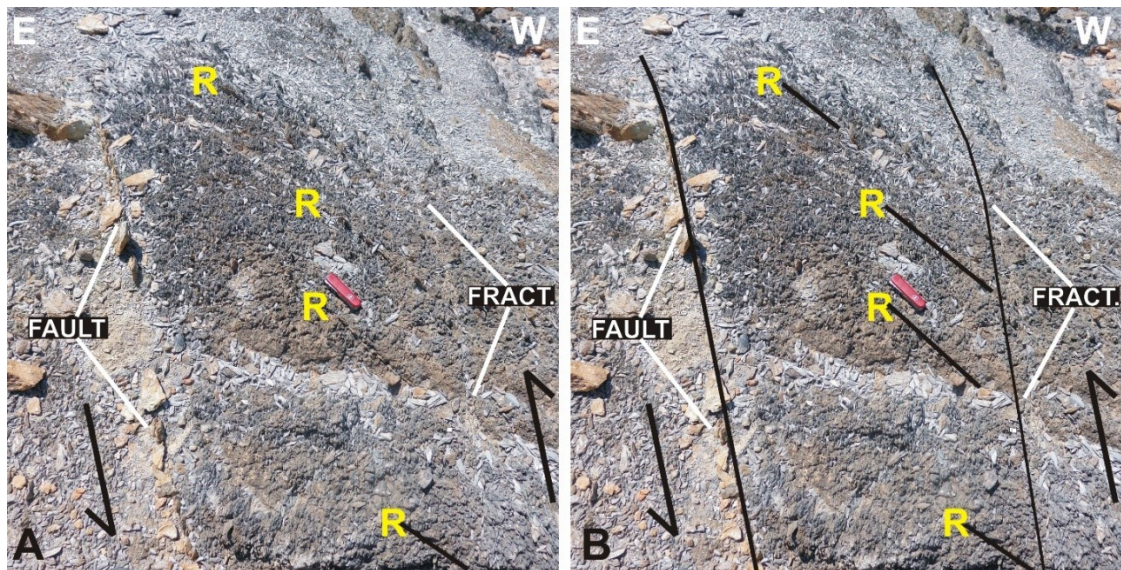


Figure 11. Sinistral calcite-filled fracture system with a minor fault (left) and a parallel fracture (right). Between the fault and the fracture is a parallel array of widened, right-stepping Riedel shears (marked by “R”). The red pocket knife for scale is positioned parallelly to the calcite shear veins. (A) Natural appearance of structures. (B) Fractures marked by black lines for easier perception.

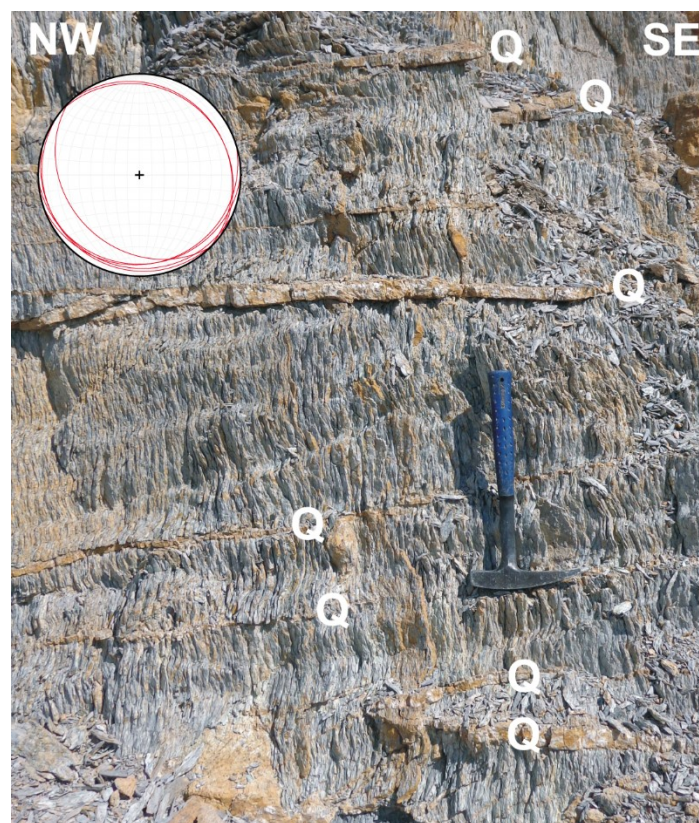


Figure 12. Gently dipping quartz veins (Q) following the scattering crenulation cleavage S_2 or displaying a similar orientation to S_2 . The Schmidt net shows the orientation of the gently dipping quartz veins.



Figure 13. Contact between the Amdeh and Hiyam formations. The contact is marked by the sinistral Wadi Amdeh Fault (dashed white line). Note the slickenlines between the two black dashed lines. The two white arrows point to the red cataclasite/tectonic breccia in close proximity to the fault. Note that the red cataclasite/tectonic breccia is obliquely oriented to the fault, being in contact with the fault in the foreground and separated from the fault in the background. Coordinates of the fault: $23^{\circ}19'45.12''\text{N}/58^{\circ}23'43.95''\text{E}$.

The contact surface of the Hiyam Formation with the Amdeh siltstones is marked by a large slickenside of the Wadi Amdeh Fault (Figure 15) which is exposed over an area of several m^2 . The slickenside is associated with the Hiyam Formation which represents the northeastern fault block (see Figure 3). It is steeply dipping to the SW ($220\text{--}225/86\text{--}88$), exhibiting horizontal slickenlines which plunge ($142/04$) and ($315/03$). Some areas of the slickenside are polished/reflective. The shear sense is sinistral as indicated by corresponding Riedel shears and decimeter scale drag folds on the northeastern fault block. The slickenlines reveal strike-slip parallel to the contact surface of both formations.

Thin section evidence shows that the material of the cataclasite/tectonic breccia is dominated by feldspar, quartz, and muscovite, indicating that it may represent a deformed felsic igneous rock. Feldspar may be highly sericitized. There are carbonate cements. By X-ray diffraction the silicates quartz, anorthoclase, as well as muscovite and kaolinite were identified, and the carbonates are represented by dolomite and ankerite (Appendix A: Figures A1–A3). The presence of anorthoclase, muscovite, and kaolinite seems to indicate the elevated presence of the alkaline elements sodium (Na) and potassium (K). An elevated concentration of potassium (K) is also manifested in six X-ray fluorescence measurements. The used XRF device does not quantify concentrations of Na.

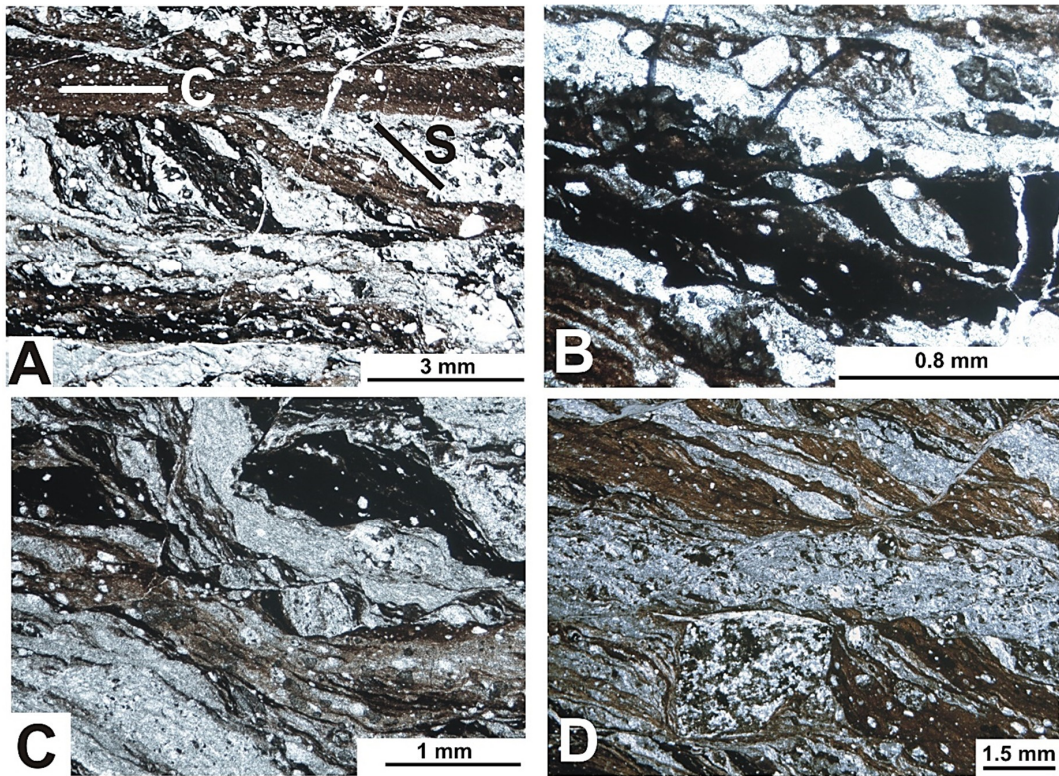


Figure 14. Thin section micrographs of the reddish cataclasite/tectonic breccia which formed at the brittle–ductile transition. Note the foliation and flow fabrics! (A) Foliated sample with S-C fabric. (B) Altered feldspar crystal in dark matrix, sheared into three fragments (center), which become larger to the right. Shearing ensued parallel to the foliation. Note that the fragments display size and shape match across the shear planes. The shear planes are mineralized (light surfaces in dark matrix; left shear plane is deformed). (C) Altered feldspar crystal, sheared into two fragments (center) parallel to the foliation. The fragments display size and shape match across the shear planes. (D) Large porphyroclast system with pressure shadows displaying stair-stepping geometry (center bottom). Moreover, note the probable synthetic shear plane displacing the foliation (upper right and upper center). The long sides of the micrographs are parallel to the main foliation. All PPL.



Figure 15. Part of the large slickenside in the Hiyam Formation of the Wadi Amdeh Fault with horizontal slickenlines (black dashed lines). The slickenside marks the contact between the Amdeh and Hiyam formations.

Although an arkose or an arkosic arenite could also be composed in the same way, we rule out that this reddish rock is a deformed sandstone because it would be unlikely for such an immature sandstone to occur as an isolated, “exotic” layer in the midst of a mature quartz-rich siltstone succession. These siltstones are compositionally mature (quartz) and texturally mature (fine-grained, well-sorted).

6. Interpretation

During the Late Cretaceous, folding took place in the subduction zone (see below). The folds were later tilted during late Cretaceous to Cenozoic doming. The orientation of the Amdeh fold axes is approximately parallel to the overall trend of the Saih Hatat Dome, whose SW margin of Mesozoic rocks was tilted by $\sim 30^\circ$ to the SW during doming (map by [15]), but this had no effect on the trend of the Amdeh fold axes and the orientation of the related shortening direction, respectively.

Our results allow us to compare the characteristics of the studied folds of the Amdeh Formation of the Saih Hatat Dome with the Cadomian and Angudan folds from the Jabal Akhdar Dome. Considering the steeply dipping axial planes and cleavage surfaces (Figure 7A,B) of the measured Amdeh folds, they cannot be attributed to the Cadomian Orogeny. Taking into account that the orientation of the studied folds is perpendicular to that of the Angudan folds, they cannot be related to the Angudan Orogeny. The lack of Cadomian and Angudan folds in the Amdeh Formation suggests that Am 1 must have accumulated after 525 ± 5 Ma (compare Figure 2). Thus, we rule out a Fortunian age as too old for Am 1 (compare Figure 2). An Upper Terrenewian age (late stage 2) could be considered.

Instead, the folds in the Amdeh Formation are related to the Semail Orogeny. The rocks of the Jabal Akhdar and Saih Hatat domes were exposed to overthrusting by the obducted rock masses during the Late Cretaceous. They were also exposed to subduction and exhumation from the subduction zone (e.g., [36,54,59]). However, the rocks of the Saih Hatat area were subducted to greater depths than those of the Jabal Akhdar region [36,47,48]. Since the Saih Hatat rocks were exposed to greater subduction depth and subsequently to a more extensive exhumation process than the Jabal Akhdar rocks, different deformation patterns between both areas can be explained. (compare [36], their Figure 4a).

The fold vergences observed in the Amdeh Formation could be related to deformation that was acquired by simple shear while descending into the subduction zone and were preserved in the process of exhumation (no or no significant shearing with opposite shear sense). Geometrically and kinematically, the fold vergences could also be explained by overthrusting of the obducted rock masses. The vergences could also have formed by a combination of both processes. However, it should be noted that no such folds have been described from siliciclastic rocks of the Jabal Akhdar Dome which were subjected to relatively shallow subduction (and only moderate exhumation). Thus, we suggest that the folds of the Saih Hatat Dome probably did not form by overthrusting/obduction as this process should have affected rocks in both domes in a similar way. Instead, the studied folds have formed more likely during Late Cretaceous subduction. Deformation related to this process is assigned to D_1 .

The folding-related cleavage is S_1 (Figures 7A, 8B and 9A). Thus, S_1 was also acquired during subduction along with folding and is also assigned to D_1 . Since there is a geometric relationship between the fold axes and S_1 , S_2 , and S_3 (Figure 7A), the three cleavage systems are related to the Semail Orogeny.

The observed thinning of fold flanks and thickening of quartzite fold hinges (Am 2) indicates ductile flow of quartz which requires certain temperature conditions. According to [60], quartz becomes ductile at 300°C . This temperature defines the upper limit of the cooling temperature estimates of $200\text{--}300^\circ\text{C}$ for Late Cretaceous burial and was determined by analyzing low-temperature geochronology rock samples from the Amdeh Formation near Wadi Qahza [50,59]. The peak temperature could have been even higher, reached within the subduction zone. This supports our interpretation that the Amdeh folds had formed during the Late Cretaceous.

S_2 has likely formed during exhumation when the subducted slab was exhumed out of the subduction channel. Deformation related to this process is assigned to D_2 . The transport direction

indicated by the asymmetric boudins is compatible with the exhumation process. Thus, we suggest that boudinage also represents D_2 .

The observation that boudins which mainly consist of reworked beige dolostone clasts of the Hiyam Formation (see [4]) occur so frequently near the Wadi Amdeh Fault is due to the fact that beds of Am 1 near the fault are the oldest exposed beds of the Amdeh Formation and their stratal proximity of the subjacent Hiyam Formation. These beds of the Amdeh Formation are expected to contain the most reworked dolostone fragments of the unconformably underlying Hiyam Formation.

The widened and steeply dipping calcite-filled faults that are paralleled by arrays of widened, right-stepping Riedel shears or tension gashes that are also calcite-filled represent a sinistral fracture. However, this system is unrelated to the sinistral Wadi Amdeh Fault as the orientation of this fracture system is neither parallel to the master fault nor to the synthetic direction within a sinistral system (Figure 16). As the shear veins are intersected/fragmented by S_3 , we suggest that this fracture system is related to unspicifiable movements related to the D_2 interval.

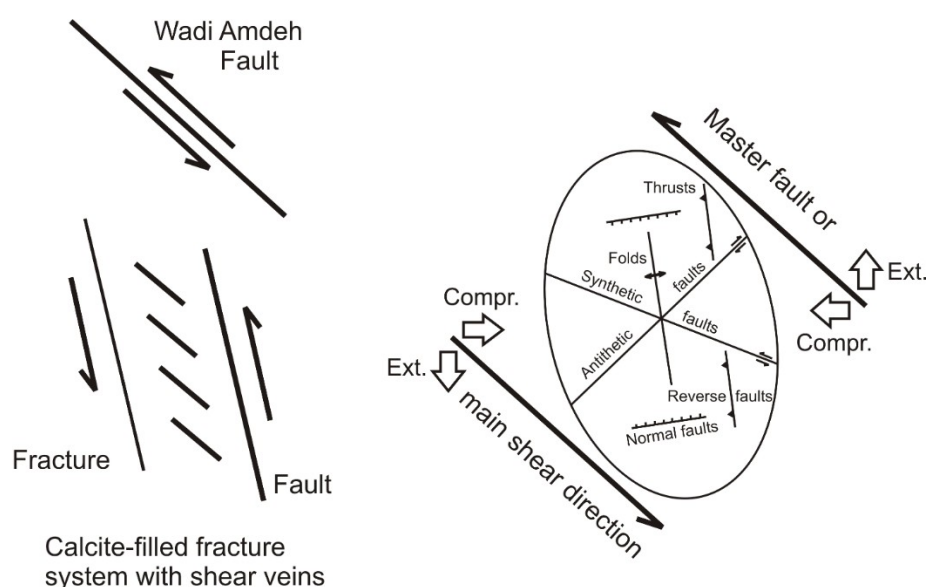


Figure 16. Geometric relationship between the Wadi Amdeh Fault (master fault) and the calcite-filled fracture system. Note that this system cannot be a synthetic element of a sinistral master fault if compared with a respective strain ellipse model (ellipse drawn after [61]).

As S_3 postdates S_1 and S_2 it must be related to a tectonic process that postdates exhumation from the subduction channel. Since the bisector of the two conjugate S_3 sets trends perpendicularly to the trend of the fold axes and parallel to the horizontal σ_1 , S_3 should be related to a late process of the Semail Orogeny. We propose that S_3 formed in the course of obduction of the Semail Ophiolite as an extensional fracture system, caused by extension perpendicularly oriented to the thrust direction. This interpretation also takes into account the conjugate arrangement of S_3 . Deformation related to this process is assigned to D_3 .

The orientations of the gently inclined quartz veins largely conform to the orientation of S_2 . There is evidence that many of these veins follow S_2 (Figure 12), and none of these veins is folded. Therefore, they postdate folding. However, there are particular differences among veins of this set as the majority of the thin veins occurs in the distinct deformation zone in proximity to the Wadi Amdeh Fault while the thickest quartz vein occurs remotely from the majority of the thin veins. The fracture of the thick vein may have opened in the course of obduction of the Semail Ophiolite after folding of the Amdeh Formation was completed. Horizontal compression may have led to local vertical extension. Deformation related to this process is assigned to D_3 . Since most of these veins (thin veins) occur in close proximity to the Wadi Amdeh Fault, we suggest that fissure formation was due to frictional

effects and/or compensation movements related to shearing along the strike-slip fault. Deformation related to this process is assigned to D_4 . Thus, we imply that similarly oriented quartz veins may have formed by two different processes.

Since D_4 represents a process that postdates folding, the paleostress analysis by [53] may provide a possible clue as to when sinistral shearing could have occurred although our study area was not included in the investigation by [53]. Taking into account that the deduced sinistral slip implies E-W compression (Figure 16), the paleostress analysis reveals that E-W compression was detected only for the Early Miocene (Figure 5). The cause of this compression is unclear [53]. The map by [15] indicates the presence of straight faults at/near Wadi Amdeh which strike similarly to the Wadi Amdeh Fault (see also Figure 6).

D_4 also includes sheared and rotated bedding and cleavage fabrics, as well as the formation of the cataclasite/tectonic breccia. The orientation of the largest fold of the study area (Figure 3) is indistinguishable from that of the other observed folds. It is intriguing that of all folds, the largest fold occurs near the Wadi Amdeh Fault and displays an axis whose orientation is also consistent with the orientation of fold axes that would form due to sinistral slip (Figure 16). Whether this is significant or not remains to be seen.

A novel discovery is the reddish cataclasite which is of felsic origin, representing a volcanic layer (or sill) within the lower part of Am 1. The alkaline character would be compatible with a rift interpretation and may indicate that rift pulses continued from the Ara rifting which is partly time equivalent to the volcanic deposits of the Fara Formation of the Jabal Akhdar Dome [6] (Figure 4) through the Cambrian to the “mid-Ordovician rift pulse” identified by [62].

7. Conclusions

The folds of the Amdeh Formation did not form during the Cadomian and Angudan orogenies. Based on our structural and paleotemperature considerations, the folds formed in the course of the Semail Orogeny, probably during Late Cretaceous subduction. Moreover, our structural findings indicate that the age of Am 1 is not equivalent to the Karim Formation. It appears possible that the age of Am 1 overlaps with the upper part of the Haradh Formation (compare Figure 2).

The contact between the Hiyam and Amdeh formations is the sinistral and almost vertical Wadi Amdeh Fault. It is not a stratigraphic contact and, thus, not an unconformity. However, the frequent occurrence of the Hiyam dolostones in the lowermost exposed parts of Am 1 may indicate a stratigraphic contact between both formations in the subsurface of the southwestern fault block, and this could well be an unconformity.

At this point, our observations and interpretations of alkaline volcanic material is only of preliminary character. Future absolute age dating and more extensive geochemical analyses will enhance our present state of knowledge. Future structural work in the Hiyam and Hatat formations (Figure 4) will clarify whether the Neoproterozoic formations of the Saih Hatat Dome were affected by the Cadomian and Angudan orogenies or not.

Author Contributions: Manuscript text, F.M., A.S., K.S., and I.C.; Illustrations, A.S. and F.M.; Field work, F.M., A.S., S.A.-W., P.-J.W., I.A., and K.S; Thin section analyses, W.-P.W., F.M., and A.S.; XRD analyses, I.A.; XRF analyses, B.P. All authors have read and agreed to the published version of the manuscript.

Funding: This research received no funding.

Acknowledgments: We thank Christoph von Hagke and Amerigo Corradetti as well as an anonymous reviewer for their constructive comments which increased the clarity of the manuscript. We also thankfully acknowledge Sarah Mattern’s review of the English text. Saja Al-Wahaibi carried out a Final Year Project as a student at Sultan Qaboos University related to the folds of the Amdeh Formation in Wadi Amdeh and Wadi Qahza. We thank the SQU technicians Hamdan Al-Zidi (Earth Science Department) and Saif Al-Mamari (Central Analytical & Applied Research Unit, CAARU) for their support in sample preparation and processing.

Conflicts of Interest: The authors declare no conflict of interest.

Appendix A

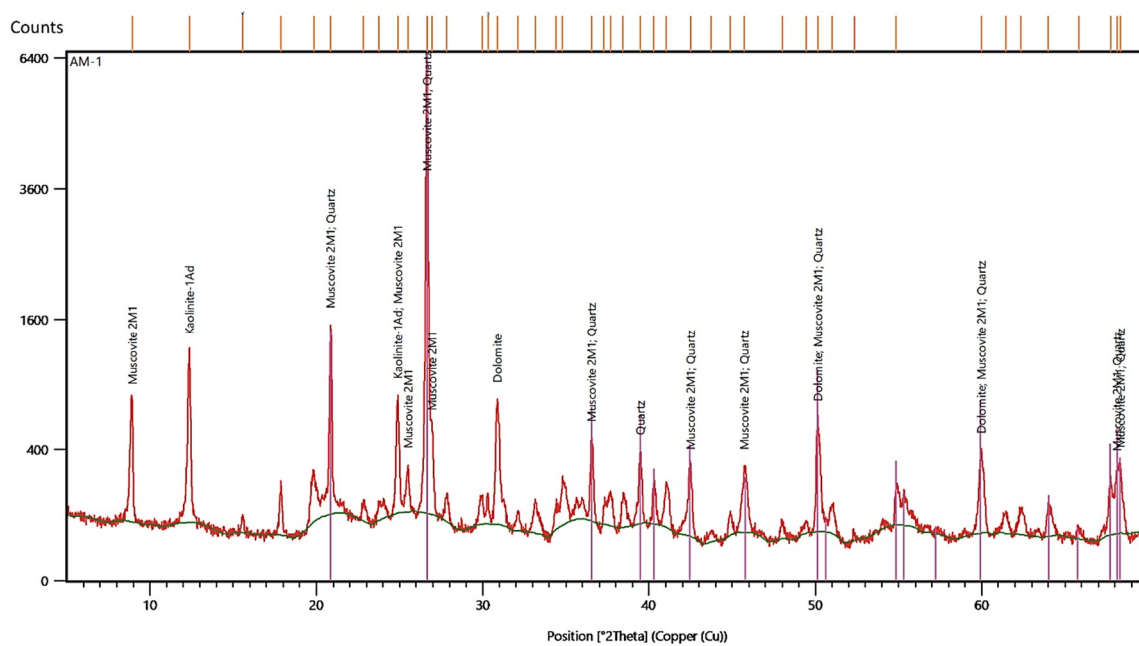


Figure A1. XRD diagram of sample Am 1 (reddish cataclasite).

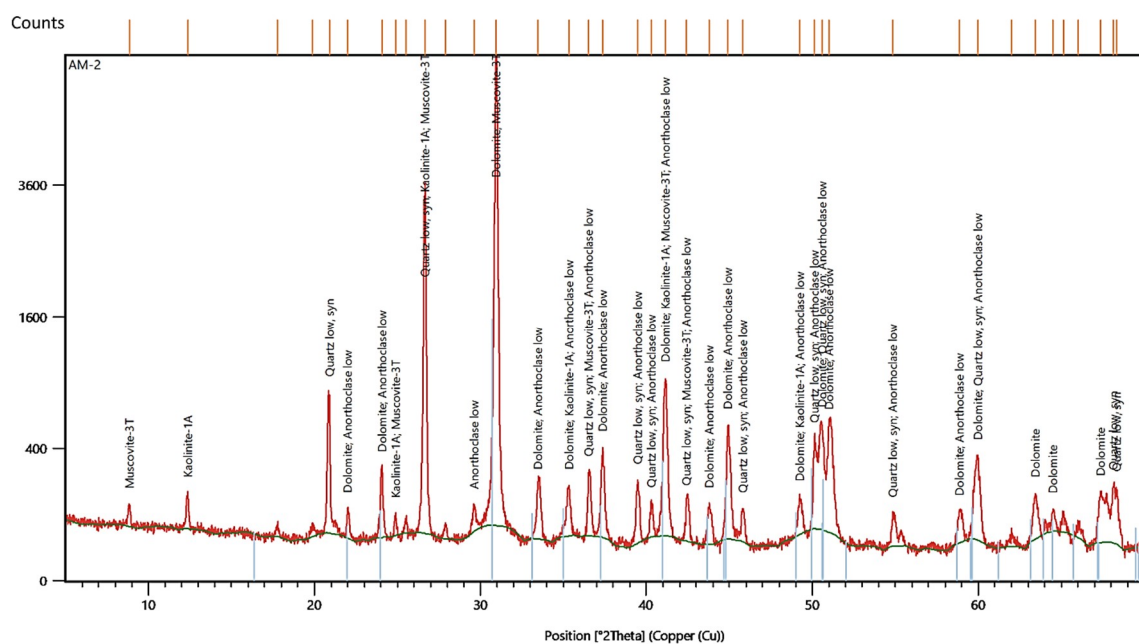


Figure A2. XRD diagram of sample Am 2 (reddish cataclasite).

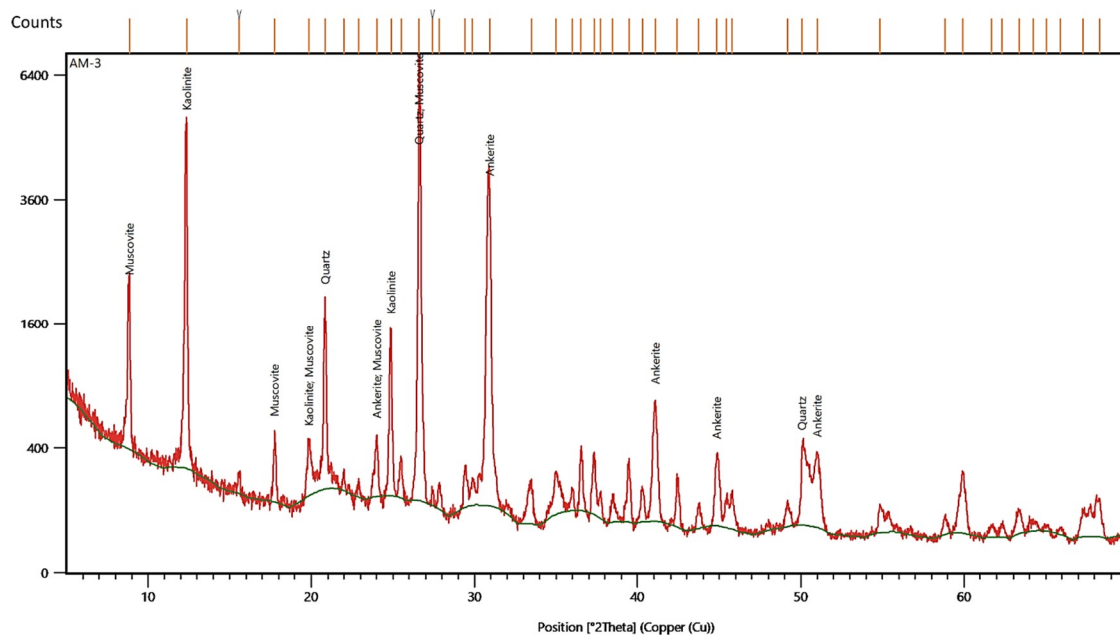


Figure A3. XRD diagram of sample Am 3 (reddish cataclasite).

References

- Callegari, I.; Scharf, A.; Mattern, F.; Bauer, W.; Pinto, A.J.; Rarivoarison, H.; Scharf, K.; Al Kindi, M. Gondwana accretion tectonics and implications for the geodynamic evolution of eastern Arabia: First structural evidence of the existence of the Cadomian Orogen in Oman (Jabal Akhdar Dome, Central Oman Mountains). *J. Asian Earth Sci.* **2020**, *187*, 104070. [[CrossRef](#)]
- Hu, P.; Zhai, Q.; Ren, G.; Wang, J.; Tang, Y. Late Ordovician high-Mg adakitic andesite in the western South China block: Evidence of oceanic subduction. *Int. Geol. Rev.* **2017**, *60*, 1140–1154. [[CrossRef](#)]
- Al-Husseini, M.I. Ediacaran-Cambrian Middle East geologic time scale 2014, proposed correlation of Oman's Abu Mahara Supergroup and Saudi Arabia's Jibalah Group. *GeoArabia* **2014**, *19*, 107–132.
- Lovelock, P.E.R.; Potter, T.L.; Walsworth-Bell, E.B.; Wiemer, W.M. Ordovician rocks in the Oman Mountains: The Amdeh Formation. *Geol. Mijnb.* **1981**, *60*, 487–495.
- Heward, A.P.; Miller, C.G.; Booth, G.A. The Early Ordovician Middle Shale Member (Am3) of the Amdeh Formation and further evidence of conodont faunas from the Sultanate of Oman. *Geol. Mag.* **2018**, *156*, 1357–1374. [[CrossRef](#)]
- Forbes, G.A.; Jansen, H.S.M.; Schreurs, J. *Lexicon of Oman Subsurface Stratigraphy: Reference Guide to the Stratigraphy of Oman's Hydrocarbon Basins*; GeoArabia Spec. Publ.: Petrolink, Bahrain, 2010; Volume 5, pp. 1–373.
- Loosveld, R.J.H.; Bell, A.; Terken, J.J.M. The tectonic evolution of interior Oman. *GeoArabia* **1996**, *1*, 28–51.
- Allen, P.A. The Huqf Supergroup of Oman: Basin development and context for Neoproterozoic glaciation. *Earth Sci. Rev.* **2007**, *84*, 139–185. [[CrossRef](#)]
- Droste, H. Petroleum geology of the Sultanate of Oman. In *Petroleum Systems of the Tethyan Region*; Marlow, L., Kendall, C., Yose, L., Eds.; Amer. Ass. Petrol. Geol. Mem.: Tulsa, Oklahoma, 2014; Volume 106, pp. 713–755.
- Le Métour, J.; Villey, M.; De Gramont, X. *Geological Map of Quryat, Sheet NF 40-4D, Scale 1:100,000. With Explanatory Notes*; Directorate General of Minerals, Oman Ministry of Petroleum and Minerals: Muscat, Oman, 1986.
- Miller, J.M.L.; Gray, D.R.; Gregory, R.T. Geometry and significance of internal windows and regional isoclinal folds in northeast Saih Hatah, Sultanate of Oman. *J. Struct. Geol.* **2002**, *24*, 359–386. [[CrossRef](#)]
- Searle, M.P.; Warren, C.J.; Waters, D.J.; Parrish, R.R. Structural evolution, metamorphism and restoration of the Arabian continental margin, Saih Hatat region, Oman Mountains. *J. Struct. Geol.* **2004**, *26*, 451–473. [[CrossRef](#)]

13. Beurrier, M.; Béchenec, F.; Rabu, D.; Hutin, G. *Geological Map of Rustaq, Sheet NF 40-3D, Scale 1:100,000, with Explanatory Notes*; Directorate General of Minerals, Oman Ministry of Petroleum and Minerals: Muscat, Oman, 1986.
14. Rabu, D.; Béchenec, F.; Beurrier, M.; Hutin, G. *Geological Map of Nakhl, Sheet NF 40-3E, Scale 1:100,000, with Explanatory Notes*; Directorate General of Minerals, Oman Ministry of Petroleum and Minerals: Muscat, Oman, 1986.
15. Villey, M.; De Gramont, X.; Le Métour, J. *Geological Map of Fanjah, Sheet NF 40-3F, Scale 1:100,000, with Explanatory Notes*; Directorate General of Minerals, Oman Ministry of Petroleum and Minerals: Muscat, Oman, 1986.
16. Béchenec, F.; Roger, J.; Le Métour, J.; Wyns, R. *Geological Map of Seeb, Sheet NF 40-03, Scale 1:250,000, with Explanatory Notes*; Directorate General of Minerals, Oman Ministry of Petroleum and Minerals: Muscat, Oman, 1992.
17. Mattern, F.; Pracejus, B.; Al Balushi, L. Heavy mineral beach placers of the Ordovician Amdeh Formation (Member 4, Wadi Qazah, Saih Hatat, eastern Oman Mountains): Where is the main source area? *J. Afr. Earth Sci.* **2018**, *147*, 633–646. [[CrossRef](#)]
18. Mattern, F.; Scharf, A. Transition from the Hajir Formation to the Muaydin Formation: A facies change coinciding with extensional, syndepositional faulting (Ediacaran, Jabal Akhdar Dome, Central Oman Mountains). *J. Afr. Earth Sci.* **2019**, *152*, 237–244. [[CrossRef](#)]
19. Scharf, A.; Mattern, F.; Moraetis, D.; Callegari, I.; Weidle, C. Postobductional Kinematic Evolution and Geomorphology of a Major Regional Structure—The Semail Gap Fault Zone (Oman Mountains). *Tectonics* **2019**, *38*, 1–23. [[CrossRef](#)]
20. Brasier, M.; McCarron, G.; Tucker, R.; Leather, J.; Allen, P.; Shields, G. New U-Pb zircon dates for the Neoproterozoic Ghubrah glaciation and for the top of the Huqf Supergroup, Oman. *Geology* **2000**, *28*, 175–178. [[CrossRef](#)]
21. Bowring, S.A.; Grotzinger, J.P.; Condon, D.J.; Ramezani, J.; Newall, M.; Allen, P.A. Geochronologic constraints of the chronostratigraphic framework of the Neoproterozoic Huqf Supergroup, Sultanate of Oman. *Am. J. Sci.* **2007**, *307*, 1097–1145. [[CrossRef](#)]
22. Immerz, P.W.; Oterdoom, H.; El-Tonbary, M. The Huqf/Haima hydrocarbon system of Oman and the terminal phase of the Pan-African Orogeny: Evaporite depositions in a compressive setting. In *Proceedings of the 4th Middle East Geosciences Conference, GEO 2000; GeoArabia: Petrolink, Bahrain, 2000; Volume 5*, pp. 113–114.
23. Koopman, A.; van der Berg, M.; Romine, K.; Teasdale, J. Proterozoic to Cambrian plate-tectonics and its control on the structural evolution of the Ara Salt-Basin in Oman. In *Proceedings of the American Association of Petroleum Geologists European Region Conference, Athens, Greece, 17–20 November 2007*.
24. Al-Kindy, M.H.; Richard, P.D. The main structural styles of the hydrocarbon reservoirs in Oman. In *Tectonic Evolution of the Oman Mountains*; Rollinson, H.R., Searle, M.P., Abbasi, I.A., Al-Lazki, A.I., Al-Kindy, M.H., Eds.; Geological Society, London, Special Publications: London, UK, 2014; Volume 392, pp. 409–445.
25. Franke, W. The mid-European segment of the Variscides: Tectonostratigraphic units, terrane boundaries and plate tectonic evolution. In *Orogenic Processes: Quantification and Modelling in the Variscan Belt*; Franke, W., Haak, V., Oncken, O., Tanner, D., Eds.; Geological Society, London, Special Publications: London, UK, 2000; Volume 179, pp. 35–61.
26. Matte, P. The Variscan collage and orogeny (480-290 Ma) and the tectonic definition of the Armorica microplate: A review. *Terra Nova* **2001**, *13*, 122–128. [[CrossRef](#)]
27. Faqira, M.; Rademakers, M.; Afifi, A. New insights into the Hercynian Orogeny, and their implications for the Paleozoic Hydrocarbon System in the Arabian Plate. *GeoArabia* **2009**, *14*, 199–228.
28. Steward, S.A. Structural geology of the Rub' Al-Khali Basin, Saudi Arabia. *Tectonics* **2016**, *35*, 2417–2438. [[CrossRef](#)]
29. Ruban, D.A.; Al-Husseini, M.I.; Iwasaki, Y. Review of Middle East Paleozoic Plate Tectonics. *GeoArabia* **2007**, *12*, 35–56.
30. Torsvik, T.H.; Cocks, L.R.M. *Earth History and Paleogeography*; Cambridge University Press: Cambridge, UK, 2017; pp. 1–317.
31. Abbo, A.; Avigad, D.; Gerdes, A. The lower crust of the Northern broken edge of Gondwana: Evidence for sediment subduction and syn-Variscan anorogenic imprint from zircon U-Pb-Hf in granulite xenolithes. *Gondwana Res.* **2018**, *64*, 84–96. [[CrossRef](#)]

32. Glennie, K.W.; Boeuf, M.G.A.; Hughes-Clarke, M.W.; Moody-Stuart, M.; Pilaar, W.; Reinhardt, B.M. *Geology of the Oman Mountains*; Royal Dutch Geological and Mining Society: Haarlem, The Netherlands, 1974; pp. 1–423.
33. Blendinger, W.; van Vliet, A.T.; Hughes Clarke, M.W. Updoming, rifting and continental margin development during the Late Paleozoic in northern Oman. In *The Geology and Tectonics of the Oman Region*; Robertson, A.H.F., Searle, M.P., Ries, A.C., Eds.; Geol. Soc., London, Spec. Publ.: London, UK, 1990; Volume 49, pp. 27–37.
34. Chauvet, F.; Dumont, T.; Basile, C. Structures and timing of Permian rifting in the central Oman Mountains (Saih Hataf). *Tectonophysics* **2009**, *475*, 563–574. [[CrossRef](#)]
35. Stampfli, G.M.; Borel, G.D. A plate tectonic model for the Paleozoic and Mesozoic constrained by dynamic plate boundaries and restored synthetic oceanic isochrons. *Earth Planet. Sci. Lett.* **2002**, *196*, 17–33. [[CrossRef](#)]
36. Breton, J.-P.; Béchenneq, F.; Le Métour, J.; Moen-Maurel, L.; Razin, P. Eoalpine (Cretaceous) evolution of the Oman Tethyan continental margin: Insights from a structural field study in Jabal Akhdar (Oman Mountains). *GeoArabia* **2004**, *9*, 41–58.
37. Rioux, M.; Garber, J.; Bauer, A.; Bowring, S.; Searle, M.; Kelemen, P.; Hacker, B. Synchronous formation of the metamorphic sole and igneous crust of the Semail ophiolite: New constraints on the tectonic evolution during. *Earth Planet. Sci. Lett.* **2016**, *451*, 185–195. [[CrossRef](#)]
38. Glennie, K.W.; Boeuf, M.G.A.; Hughes-Clarke, M.W.; Moody-Stuart, M.; Pilaar, W.F.H.; Reinhardt, B.M. Late Cretaceous nappes in Oman Mountains and their geological evolution. *Am. Assoc. Petrol. Geol. Bull. Tulsa (Oklahoma)* **1973**, *57*, 5–27.
39. Searle, M.P.; Malpas, J. Structure and metamorphism of rocks beneath the Semail ophiolite of Oman and their significance in ophiolite obduction. *Trans. R. Soc. Edinb.* **1980**, *71*, 247–262. [[CrossRef](#)]
40. Lippard, S.J.; Shelton, A.W.; Gass, I.G. The ophiolite of northern Oman. *J. Geol. Soc. Lond. Mem.* **1986**, *11*, 1–178.
41. Searle, M.; Cox, J. Tectonic setting, origin, and obduction of the Oman ophiolite. *Geol. Soc. Am. Bull.* **1991**, *111*, 104–122. [[CrossRef](#)]
42. Hacker, B.R.; Mosenfelder, J.L.; Gnos, E. Rapid emplacement of the Oman ophiolite: Thermal and geochronologic constraints. *Tectonics* **1996**, *15*, 1230–1247. [[CrossRef](#)]
43. Goffé, B.; Michard, A.; Kienast, J.R.; LeMer, O. A case of obduction related high pressure, low temperature metamorphism in upper crustal nappes, Arabian continental margin, Oman: P-T paths and kinematic interpretation. *Tectonophysics* **1988**, *151*, 363–386. [[CrossRef](#)]
44. Glennie, K.W. *The Geology of the Oman Mountains: An Outline of Their Origin*, 2nd ed.; Scientific Press: Beaconsfield, QC, Canada, 2005; pp. 1–110.
45. El-Shazly, A.K.; Coleman, R.G. Metamorphism in the Oman Mountains in relation to the Semail Ophiolite emplacement. In *The Geology and Tectonics of the Oman Region*; Robertson, A.H.F., Searle, M.P., Ries, A.C., Eds.; Geological Society, London, Special Publications: London, UK, 1990; Volume 49, pp. 473–493.
46. Cornish, S.; Searle, M. 3D geometry and kinematic evolution of the Wadi Mayh sheath fold, Oman, using detailed mapping from high-resolution photography. *J. Struct. Geol.* **2017**, *101*, 26–42. [[CrossRef](#)]
47. Grobe, A.; Virgo, S.; von Hagke, C.; Urai, J.L.; Littke, R. Multiphase structural evolution of a continental margin during obduction orogeny: Insights from the Jebel Akhdar Dome, Oman Mountains. *Tectonics* **2018**, *37*, 888–913. [[CrossRef](#)]
48. Grobe, A.; von Hagke, C.; Littke, R.; Dunkl, I.; Wübbeler, F.; Muchez, P.; Urai, J.L. Tectono-thermal evolution of Oman’s Mesozoic passive continental margin under the obducting Semail Ophiolite: A case study of Jebel Akhdar, Oman. *Solid Earth* **2019**, *10*, 149–175. [[CrossRef](#)]
49. Nolan, S.C.; Skelton, P.W.; Clissold, B.P.; Smewing, J.D. Maastrichtian to Early Tertiary stratigraphy and paleogeography of the Central and Northern Oman Mountains. In *The Geology and Tectonics of the Oman Region*; Robertson, A.H.F., Searle, M.P., Ries, A.C., Eds.; Geological Society, London, Special Publications: London, UK, 1990; Volume 49, pp. 307–325.
50. Hansman, R.J.; Ring, U.; Thomson, S.N.; den Brock, B.; Stübner, K. Late Eocene uplift of the Al Hajar Mountains, Oman, supported by stratigraphic and low-temperature thermochronology. *Tectonics* **2017**, *36*, 3081–3109. [[CrossRef](#)]
51. Corradetti, A.; Spine, V.; Tavani, S.; Ringenbach, J.C.; Sabbatino, M.; Razin, P.; Laurent, O.; Brichau, S.; Mazzoli, S. Late-stage tectonic evolution of the Al-Hajar Mountains, Oman: New constraints from Palaeogene sedimentary units and low-temperature thermochronometry. *Geol. Mag.* **2019**, 1–14. [[CrossRef](#)]

52. Mann, A.; Hanna, S.S.; Nolan, S.C. The post-Campanian tectonic evolution of the Central Oman Mountains: Tertiary extension of the Eastern Arabian Margin. In *The Geology and Tectonics of the Oman Region*; Robertson, A.H.F., Searle, M.P., Ries, A.C., Eds.; Geological Society, London, Special Publications: London, UK, 1990; Volume 49, pp. 549–563.
53. Fournier, M.; Lepvrier, C.; Razin, P.; Jolivet, L. Late Cretaceous to Paleogene post-obduction extension and subsequent Neogene compression in the Oman Mountains. *GeoArabia* **2006**, *11*, 17–40.
54. Searle, M.P. Structural geometry, style and timing of deformation in the Hawasina Window, Al Jabal al Akhdar and Saih Hatat culminations, Oman Mountains. *GeoArabia* **2007**, *12*, 99–130.
55. Mattern, F.; Scharf, A. Postobductional extension along and within the Frontal Range of the Eastern Oman Mountains. *J. Asian Earth Sci.* **2018**, *154*, 369–385. [[CrossRef](#)]
56. Clar, E. Ein zweikreisiger Geologen- und Bergmannskompaß zur Messung von Flächen und Linearen (Mit Bemerkungen zu den feldgeologischen Messungsarten). *Verh. Geol. Bundesanst. Wien* **1954**, 201–215.
57. Wallbrecher, E.; Unzog, W. *Gefüge 3: Ein Programmpaket zur Behandlung von Richtungsdaten*, University of Graz: Graz, Austria, 2013.
58. Béchenec, F.; Le Métour, J.; Platel, J.P.; Roger, J. *Geological Map of the Sultanate of Oman (GIS version), Scale 1:250,000*; Directorate General of Minerals, Oman Ministry of Petroleum and Minerals: Muscat, Oman, 1993.
59. Saddiqi, O.; Michard, A.; Goffé, B.; Poupeau, G.; Oberhänsli, R. Fission-track thermochronology of the Oman Mountains continental widows, and current problems of tectonic interpretation. *Bull. Soc. Géol.* **2006**, *3*, 127–134. [[CrossRef](#)]
60. Schofield, D.I.; D'Lemos, R.S. Relationship between syn-tectonic granite fabrics and regional PTtd paths: An example from the Gander-Avalon boundary of NE Newfoundland. *J. Struct. Geol.* **1998**, *20*, 459–471. [[CrossRef](#)]
61. Harding, T.P. Petroleum traps associated with wrench faults. *Am. Assoc. Petrol. Geol. Bull.* **1974**, *58*, 1290–1304.
62. Oterdoom, W.H.; Worthing, M.A.; Partington, M. Petrological and Tectonostratigraphical Evidence for a Mid Ordovician Rift Pulse on the Arabian Peninsula. *GeoArabia* **1999**, *4*, 467–500.



© 2020 by the authors. Licensee MDPI, Basel, Switzerland. This article is an open access article distributed under the terms and conditions of the Creative Commons Attribution (CC BY) license (<http://creativecommons.org/licenses/by/4.0/>).